Environ. Sci. Technol. **2009,** *43,* 4340–4347

Escherichia coli O157:H7 Transport in Saturated Porous Media: Role of Solution Chemistry and Surface Macromolecules

HYUNJUNG N. KIM,[†] SCOTT A. BRADFORD,[‡] AND SHARON L. WALKER*,[†]

Department of Chemical and Environmental Engineering, University of California, Riverside, California 92521, and U.S. Salinity Laboratory, ARS, U.S. Department of Agriculture, Riverside, California 92507

Received September 13, 2008. Revised manuscript received April 9, 2009. Accepted April 13, 2009.

The transport and deposition behavior of *Escherichia coli* O157:H7 was investigated in saturated packed-bed columns and micromodel systems over a range of ionic strength (IS) (1, 10, and 100 mM) and pH (5.8, 8.4, and 9.2) conditions. At a given IS, elevated solution pH resulted in decreased deposition as a result of the increase in the measured zeta potential of the quartz sand. This deposition trend was consistent with predictions from classic Derjaguin−Landau−Verwey−Overbeek (DLVO) theory. Conversely, the *E. coli* O157:H7 deposition was inversely proportional to IS (1−100 mM) at high pH conditions (8.4 and 9.2), whereas no effect of IS was observed at pH 5.8. This deposition trend was not consistent with DLVO theory, but could be explained by *pH-associated electrosteric stabilization*. This phenomenon is driven by the pH-dependent protonated state of functional groups on *E. coli* O157:H7 surface macromolecules and the corresponding conformational state of the bacterial polymers. Results from this study demonstrate that retention of *E. coli* O157:H7 cells in porous media is a complex process that depends on the solution chemistry, cell−cell interactions, and pore structure. The findings in this study also imply that previous work conducted at lower pH and IS conditions may underestimate *E. coli* O157:H7 travel distance in higher salt and pH groundwater environments.

Introduction

Groundwater contamination, caused by the migration of pathogenic bacteria through soil, leads to almost half of the outbreaks of waterborne diseases each year in the United States (U.S.) (*1*). Among numerous pathogens, *Escherichia coli* O157:H7, a gram-negative bacterium, is reported to be responsible for severe diarrhea (hemorrhagic colitis) and hemolytic-uremic syndrome (*2*), leading to approximately 75 000 infections and 61 deaths per year in the U.S. (*3*). It has been reported that cattle are an important host for this virulent *E. coli* strain, and that most human infections originate from contact with contaminated water, meat, vegetables, etc. (*4*). Accordingly, the highly pathogenic nature of this organism demands a clear understanding of its transport and fate in subsurface environments in order to assess and mitigate the potential risk to public health. Although much research has been conducted to investigate physical and chemical factors influencing bacterial transport in well-defined systems (e.g., refs *5* and *6*), considerably less is known about complex biological factors that also influence bacteria transport.

Classic Derjaguin−Landau−Verwey−Overbeek (DLVO) (*7, 8*) and extended DLVO (XDLVO) theories (*9*) have been extensively used to interpret the deposition mechanism of colloids and bacteria (e.g., refs *10* and *11*). Recent research has indicated that the classic DLVO and XDLVO theories are not always valid to predict microbial interactions due to the presence of complex polymer layers extending into the liquid medium (e.g., refs *12*−*14*). Depending on the solution ionic strength (IS), the presence of large macromolecules or other polymeric substances may influence the extent of microbial adhesion due to electrosteric interactions (e.g., refs *12*−*14*) which are not considered in DLVO nor XDLVO theories (*14, 15*).

Several studies have investigated the role of microbial surface macromolecules in cell adhesion under controlled conditions via atomic force microscopic methods (e.g., refs *16*−*18*), batch adhesion tests (e.g., refs *19*−*21*), radial stagnation point flow systems (e.g., refs *12, 15, 22*), and packed-bed columns (e.g., refs *19, 21, 23*). These studies indicate that surface macromolecules may enhance (*12, 20, 23*) or hinder (*15, 20*−*22*) adhesion to different types of abiotic surfaces, and that surface macromolecules can play a significant role on microbial deposition.

Some work has been conducted to investigate the coupled role of solution chemistry and cell polymers on microbe adhesion (*15, 16, 24, 25*). Studies have revealed that the presence of a divalent cation (Ca^{2+}) can substantially enhance the rate of cell deposition due to conformational changes of polymers that are induced by charge neutralization and ion bridging mechanisms (e.g., refs *25* and *26*). However, it was observed that the extent of deposition decreased at a high salt concentration (*25, 27*), implying steric stabilization was induced by IS regardless of the ions' valence. Additionally, it has been reported that the relative amount of exposed surface functional groups and the corresponding localized charge heterogeneity can influence bacterial deposition behavior (*28*), suggesting that bacterial acid–base properties, linked to the aquatic condition, may also be important in conformational change of polymers. However, the effect of pH and/or IS on a cell adhesion has typically been assumed to be less significant than ion valence (*15, 16, 24*). The aim of this study is to investigate the coupled role of IS and pH on *E. coli* O157:H7 transport and deposition in porous media. For this purpose, transport experiments were carried out in saturated packed-bed columns over a range of pH (5.8, 8.4, and 9.2) and IS (1, 10, and 100 mM) representative of groundwater conditions.

Materials and Methods

Bacterium and Solution Chemistry. *E. coli* O157:H7/pGFP strain 72 (*5*) was used in transport experiments conducted over a wide range of pH and IS conditions found in groundwater (*29, 30*). Information about the bacterial growth and preparation is found in the Supporting Information (SI). Three pH (5.8, 8.4, and 9.2) and IS (1, 10, and 100 mM) values were chosen as representative experimental conditions. A carbonate buffer (a mixture of 9×10^{-4} M $NaHCO_3$ and 1×10^{-4} M Na_2CO_3) (*31*) was utilized to increase the pH of the

* Corresponding author phone: (951) 827-6094; fax (951) 827-5696; e-mail: swalkar@engr.ucr.edu.
[†] University of California.
[‡] U.S. Department of Agriculture.

10.1021/es8026055 CCC: $40.75
Published on Web 05/07/2009

TABLE 1. Electrokinetic Properties of Quartz and *E. coli* O157:H7 Cells as well as Column Mass Balance Information[a]

pH	ionic strength (mM)	zeta potential of quartz (mV)[b]	electrophoretic mobility of cells (μm V s^{-1} cm^{-1})[c]	M_{eff} (%)	M_{sand} (%)	M_{total} (%)
5.8	1	−55.1	−0.073	20.4[d]	38.9	59.3
	100	−16.0	−0.112	1.9	57.4	59.3
8.4	1	−55.4	−0.262	2.7	88.1	90.8
	10	−41.8	−0.148	21.4	55.9	77.3
	100	−23.7	−0.232	100.3	2.0	102.3
9.2	1	−63.8	−0.168	32.9	54	86.9
	10	−53.5	−0.167	103.7	8.6	112.3
	100	−29.8	−0.462	102.9	5.0	107.9

[a] Here, M_{eff}, M_{sand}, and M_{total} refer to the effluent, retained, and total percentage of *E. coli* O157:H7 cells recovered from column experiments, respectively. All values represent the relative percentage of the cells by number. M_{eff} was determined by integrating beneath the effluent concentration profile in Figure 1. M_{sand} was determined from the experimentally determined deposition profile in Figure 2. [b] Average value obtained from SI Figure S3. [c] Average value obtained from SI Figure S1a. [d] Value including the amount eluted by first and second flow interruption (each 0.4% of cells eluted), and DI water flush (18.7% eluted).

solution, except for an unadjusted electrolyte solution at pH 5.8. As needed, the final pH was adjusted using either 0.1 N HCl or NaOH solution (changes in the IS due to pH adjustment were negligible). The IS of the solutions was adjusted using KCl as the background electrolyte. The solution pH was measured (ϕ 350 pH/Temp/mV Meter, Beckman Coulter, Fullerton, CA) and the IS was calculated. All chemicals were reagent grade (Fisher Scientific).

Cell Characterization. Cell viability, size, shape, electrophoretic mobility, and hydrophobicity were evaluated as a function of pH and IS at 0 h and compared to similar data measured after 3 h of cell acclimation in the desired electrolyte. The results are presented in SI Table S1, Figures S1 and S2. This acclimation time was selected based on the length of the time of the column experiments to determine whether there were any physiological changes in the cells. The experimental details for the cell characterization are provided in the SI. The viability results show that the percentage of viable cells at 0 and 3 h was greater than or equal to 87 and 80%, respectively, with no statistical difference at given solution conditions ($P > 0.01$) (SI Table S1). The average effective cell diameter was approximately 0.72 ± 0.02 μm over the pH and IS ranges investigated for 0 and 3 h acclimated cells (SI Table S1). Statistical differences were observed at certain conditions ($P < 0.01$); however, no strong relationship between the change in cell size and the observed transport behavior was found at given conditions. The average aspect ratio also ranged from 2.8 ± 1.6 (minimum) to 3.7 ± 2.2 (maximum) with no significant difference regardless of solution conditions and acclimation time ($P > 0.01$) (SI Table S1). Additionally, the cells showed similar mobility values and they were relatively hydrophilic over the IS and pH ranges investigated regardless of acclimation time (SI Figures S1 and S2). Hence, cell die-off and changes in cell size, shape, mobility, or hydrophobicity are not significant parameters.

Porous Media. Ultrapure quartz sand (Iota quartz, Unimin Corp., NC) was utilized as the porous medium for the transport experiments. Sand preparation procedures are discussed in the SI. The average sand diameter (d_{50}) was approximately 275 μm. The gravimetrically measured bed porosity was determined to be ca. 0.47. In order to characterize the electrokinetic properties of the porous medium, the streaming potential of the quartz sand was measured as a function of pH and IS using an Electro Kinetic Analyzer (EKA) (Anton Paar GmbH, Graz, Austria) equipped with a cylindrical cell (*32*) and this information is presented in Table 1 and SI Figure S3.

Column Experiments. An adjustable chromatography column (Omnifit, Boonton, NJ) with a 1.5 cm inner diameter and a length of 10 cm was used for transport experiments. The superficial velocity was maintained at 0.1 cm min^{-1} for all experiments. A pulse of bacteria suspension, at a concentration of 5×10^8 cells mL^{-1}, was injected into the column for four pore volumes (PV), followed by a bacteria free electrolyte solution (>20 PV). The profile for *E. coli* O157:H7 cells retained in the column was obtained after recovery of the breakthrough curve (BTC) (*5*). The effluent and retained cell concentrations were measured using a spectrophotometer (SP-890, Barnstead International, Dubuque, IA) and fluorometer (FM109545, Barnstead International, Dubuque, IA), respectively. The total percentage of recovered cells (M_{total}) was calculated from percentages in the effluent (M_{eff}) and within the sand (M_{sand}). Additional information about the column experiments is provided in the SI.

Micromodel Experiments. In order to visually examine the deposition of *E. coli* O157:H7 cells in the quartz sand, a few representative transport experiments were conducted in a specially designed micromodel. The detailed information regarding the micromodel system can be found elsewhere (*5, 33*) and in the SI. The *E. coli* O157:H7 suspension was injected to the chamber at an approach (Darcy) velocity of 0.1 cm min^{-1}. During and after micromodel experiments, the deposition behavior of the fluorescent *E. coli* O157:H7 cells was microscopically examined.

Numerical Modeling. Some of the cell BTCs were simulated using the HYDRUS 1D computer software (*34*) in order to better interpret mechanisms of cell retention and transport. The cell transport equations that were solved are provided in the SI and the fitted model parameters are summarized in SI Table S2.

Results and Discussion

Observed Bacterial Transport and Deposition Behavior. *(a) BTCs.* Figure 1 shows the BTCs for *E. coli* O157:H7 cells as a function of IS at pH 5.8, 8.4, and 9.2. Almost no difference in effluent cell concentration with IS was observed at pH 5.8 (i.e., in Figure 1a 0.9 and 1.9% of injected cells eluted for 1 and 100 mM, respectively). In contrast, at the higher pH conditions (i.e., 8.4 and 9.2) cell retention was inversely proportional to IS (Figures 1b and c). Comparison of panels a−c of Figure 1 reveals that the amount of *E. coli* O157:H7 cells exiting the column increased with pH for a given IS. Mass balance results presented in Table 1 indicate that for a pH of 5.8, 8.4, and 9.2 the cell breakthrough was observed to be 0.9, 2.7, and 32.9% when the IS was 1 mM, and 1.9, 100.3, and 102.9% when the IS was 100 mM, respectively. Similarly, 21.4 and 103.7% of the injected cells came out of the column when the IS was 10 mM and the pH was 8.4 and 9.2, respectively.

(b) Deposition Profiles. Figure 2 presents the corresponding deposition profiles of *E. coli* O157:H7 cells retained in the column as a function of dimensionless depth. Observed

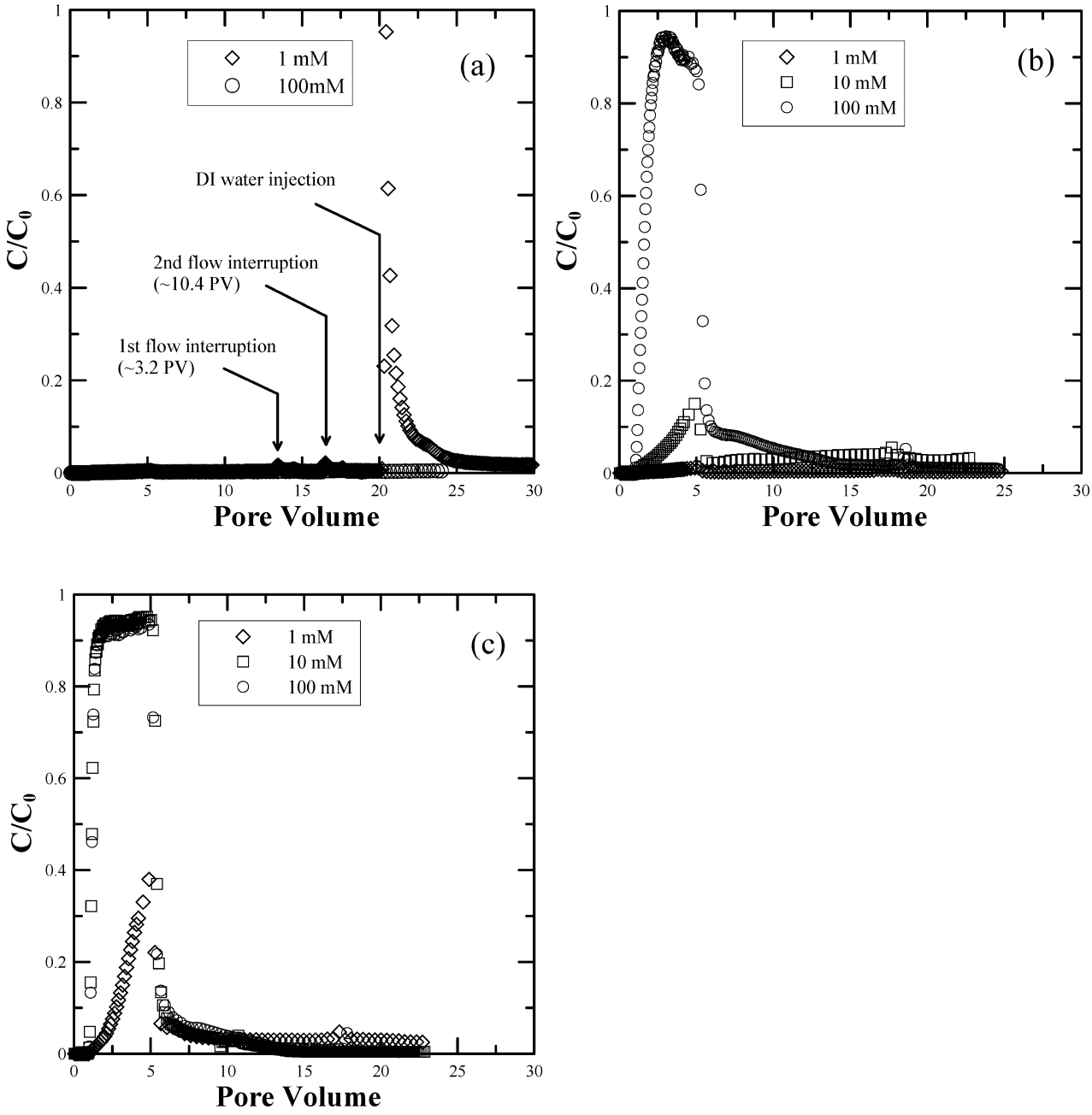

FIGURE 1. Representative BTCs for *E. coli* O157:H7 as a function of IS at (a) pH 5.8, (b) pH 8.4, and (c) pH 9.2. For the experiment conducted at 1 mM in (a), flow interruption was carried out twice, followed by DI water flush.

trends with respect to the cell retention as a function of pH and IS were consistent with the BTC data discussed above. The amount of cell deposition did not monotonically decrease with distance from the top of the column as predicted by irreversible attachment (*35*) or straining (*36*) models. Specifically, a nonmonotonic decrease in cell concentration with depth was observed. In systems with the greatest amount of cell retention a sharp peak in concentration occurred around a dimensionless depth of 0.1 (i.e., 100 mM at pH 5.8 and 1 mM at pH 8.4). Conversely, in systems with lower amounts of cell retention (i.e., 10 mM at pH 8.4, and 1 mM at pH 9.2) these peaks tended to be broader and flatter.

(c) Micromodel Experiments. Additional transport experiments were conducted using a specially designed micromodel to complement column results with the *E. coli* O157:H7 cells. SI Figure S4 show the images captured at different experimental conditions (1 mM at pH 5.8 and pH 9.2, and 100 mM at pH 9.2). As shown in SI Figure S4, the results obtained from micromodel experiments were qualitatively consistent with those from the column study. Virtually no attachment was observed at 100 mM and pH 9.2 while a substantial amount of bacteria attached to quartz surfaces at 1 mM and pH 5.8, thus, indicating that the conditions tested were relatively unfavorable and favorable for the interaction between the cells and the quartz surfaces, respectively. Additionally, it was observed that a relatively small amount of bacteria were retained in quartz media at 1 mM and pH 9.2 compared with the results at 1 mM and pH 5.8. This was identified by the notably lower levels of cells visualized in the field of view.

Interpretation of *E. coli* O157:H7 Transport and Retention. The observed transport and retention behavior for *E. coli* O157:H7 shown in Figures 1, 2, and SI Figure S4 indicate a complex dependence on solution chemistry (pH and IS). Previous research also indicates that *E. coli* O157:H7 retention in porous media will be strongly coupled to the pore space geometry and will depend on cell−cell interactions (*5*). Each

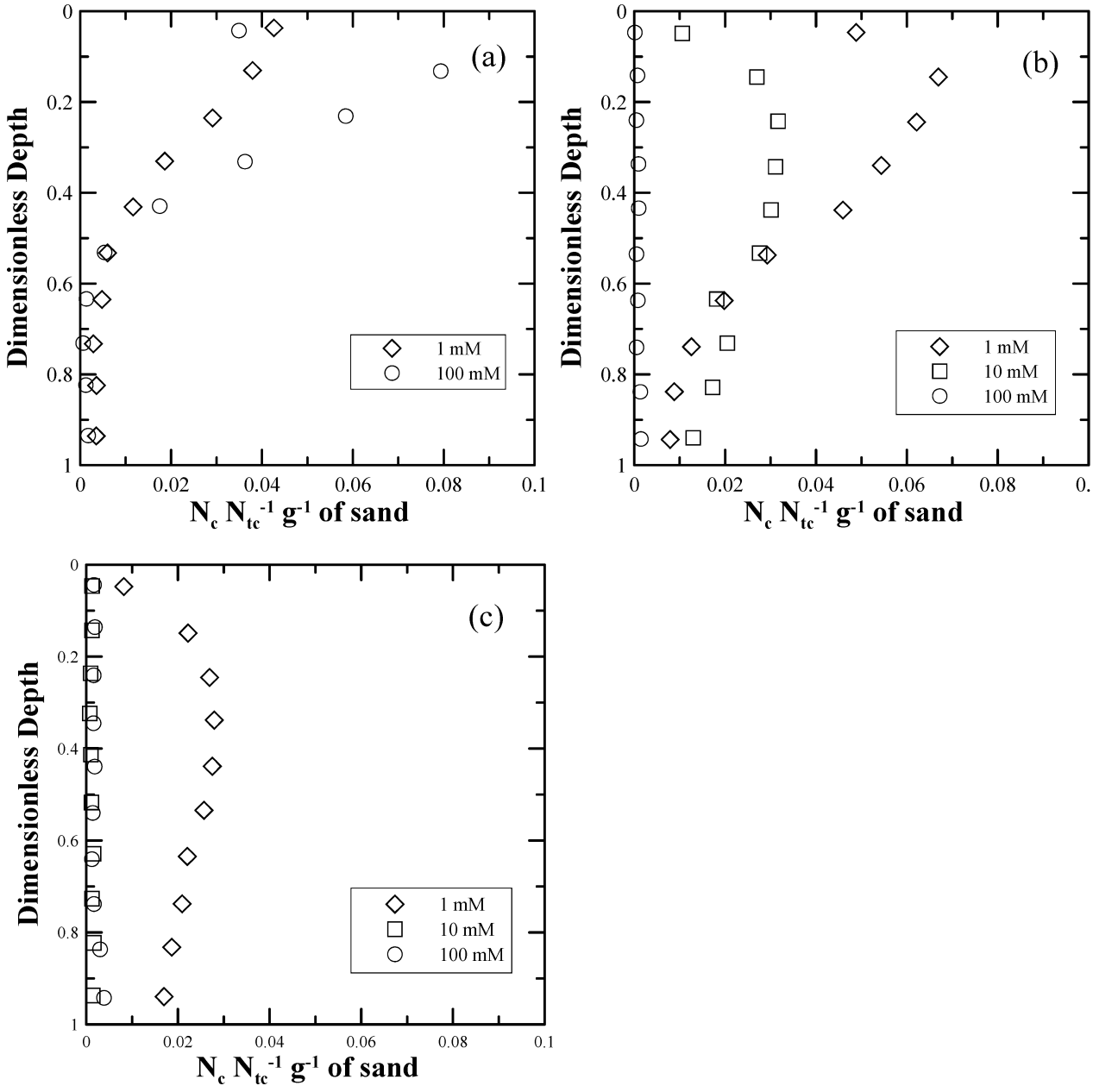

FIGURE 2. Representative deposition profiles for *E. coli* O157:H7 as a function of IS at (a) pH 5.8 (unadjusted), (b) pH 8.4, and (c) pH 9.2. The deposition profile at 1 mM in (a) was obtained after two consecutive flow interruptions and DI water flush. For (b) and (c), a carbonate buffer (a mixture of $NaHCO_3$ and Na_2CO_3) was used to increase pH and the IS was adjusted using a KCl solution except for 1 mM. The X-axis represents the normalized concentration of the cells (the number of cells in each section (~1 cm interval) of column, N_c, divided by the total number injected into the column, N_{tc}) per gram of dry sand.

of these factors will be considered below to provide a meaningful interpretation to the collected data.

(a) Solution Chemistry. Table 1 provides measured zeta potentials for the quartz grains as a function of pH and IS. The zeta potential of the grains was observed to become more negative with decreasing IS and increasing pH due to expansion of the diffuse double layer and dissociation of proton groups, respectively (*39*). In contrast, the electrophoretic mobility of the *E. coli* O157:H7 cells was relatively insensitive to changes ($P > 0.01$) in pH and IS over these same ranges, with a value of approximately -0.15 μm V s^{-1} cm^{-1} (Table 1). As mentioned in the introduction, quantitative application of DLVO theory to predict cell-sand interactions is problematic because of the presence of surface macromolecules and the fact that the cells are rod shaped. Qualitatively, DLVO theory predicts increasing cell-sand interactions with decreasing pH and increasing IS. Consistent with DLVO theory, Figures 1 and 2 indicate that cell retention at a given IS increased with decreasing pH. In this case, the zeta potential of the sand decreased with decreasing pH (Table 1) and consequently lowered the energy barrier (electrostatic repulsion) to deposition in the primary minimum (Φ_{1min}) and/or enhanced the depth of the secondary minima (Φ_{2min}) that acted on the cells near the grain surfaces.

Mass balance results presented in Table 1 suggest that approximately 40% of the cells were irreversibly retained in a Φ_{1min} type interaction at pH 5.8 for both 1 and 100 mM conditions. Figure 1a indicates that approximately 20% of the bacteria were eluted from the column by switching to deionized (DI) water, indicating that only 20% of the cells were reversibly retained in a Φ_{2min} type interaction at pH 5.8. Hence, irreversible and reversible attachment played a dominant role in cell retention at pH 5.8 when the IS was 1 and 100 mM. Conversely, retention of the remaining 40% of

the cells is still unexplained under these conditions, and this finding implies that other cell retention mechanisms were also involved. For higher pH conditions (pH 8.4 and 9.2) mass balance information presented in Table 1 indicates that irreversible cell retention was less likely (relatively good mass balance) and that unfavorable attachment conditions existed. In these cases, reversible attachment of cells is still possible but is expected to be less significant than that observed for the pH 5.8 and 1 mM system (19%).

Figures 1 and 2 indicate that cell retention at pH 8.4 and 9.2 decreased with increasing IS. This trend was not anticipated by classic DLVO theory, which most previous transport studies have reported (e.g., refs *37* and *38*). According to DLVO theory, particle deposition in porous media should increase with IS due to the reduction of electrostatic force between particles and grain surfaces (*39*). Our results show the exact opposite trend at pH 8.4 and 9.2, indicating that non-DLVO acid−base interactions were likely involved under these conditions. Possible explanations for these observations include hydrophobic interactions, an anion valence effect, and steric stabilization. Information presented in the SI indicates that hydrophobic interactions and anion valence effect are unlikely to explain this behavior. Below we discuss the potential influence of steric stabilization.

Recent studies indicate that electrosteric force can play a significant role on microbial adhesion to abiotic surfaces due to conformational changes of the polyelectrolyte layers with various functional groups (e.g., refs *15, 22)*. As discussed by Kuznar and Elimelech (*15, 22*), the presence of surface macromolecules on *Cryptosporidium* oocyst walls can considerably hinder the deposition rate on a quartz surface. They attributed this phenomenon to electrosteric repulsion; however, no direct effect of salt concentration on steric stabilization was observed (*15, 22*). Li and McLandsborough (*27*), on the other hand, observed decreasing adhesion efficiency for *E. coli* O157:H7 (EC01) cells to beef muscle over a range of IS (i.e., 1.5−150 mM PBS). Chen and Walker (*25*) observed a similar trend in adhesion experiments using *Halomonas pacifica* g in the presence of $CaCl_2$ at IS > 300 mM.

Recall that *E. coli* O157:H7 deposition was inversely proportional to IS (1−100 mM) at high pH conditions (8.4 and 9.2), whereas no effect of IS was observed at pH 5.8 (Figure 1). Results from the Figures 1 and 2 at pH 8.4 and 9.2 are consistent with the literature cited above and imply *pH-associated electrosteric stabilization* in our experiments. Previously reported titration data for *E. coli* O157:H7 cells indicated that the p*K*a values (pK_1−pK_4) are 3.25, 5.14, 7.12, and 8.70, respectively, for carboxylic and/or phosphoric groups, carboxylic group, phosphoric group, and amine or hydroxyl groups, respectively (*40*). Since the pH values employed in this study are 5.8, 8.4, and 9.2, the pH change is likely to be associated with protonation/deprotonation of the corresponding functional groups exposed on the bacterial surface polymers. Hence, we postulate that increasing the pH led to a greater degree of deprotonation of the corresponding functional groups (e.g., carboxylic and some phosphoric groups at pH 5.8, all carboxylic and phosphoric groups at pH 8.4, and all functional groups at pH 9.2), allowing for subsequent conformational change of the surface macromolecules, and consequently greater penetration of counterions in the polymer layer that enhanced repulsive interaction between the *E. coli* cells and the quartz.

One apparent discrepancy in this explanation is the reported insensitivity of the electrophoretic mobility values for *E. coli* O157:H7 cells to pH (Table 1). The disparity can be explained based upon previous studies (*22, 24*). Kuznar and Elimelech observed a significant difference in deposition rate between surface-treated and untreated oocysts, suggesting a change in the acidic nature of the surface, even though the mobility values were almost identical (*22*). Another study reported that the mobility values of bacteria harvested at different growth phases were identical even though the surface charge density (i.e., acidity) and the deposition rate to quartz surfaces were considerably different (*28*). These observations and our titration data (*40*) suggest that mobility measurement can be insensitive to detection of changes in the amount and distribution of functional groups on cell surfaces that can influence deposition behavior.

(b) Cell−Cell Interactions and Pore Structure. It is known that *E. coli* O157:H7 is capable of cell−cell interactions leading to the formation of biofilms under certain environmental conditions (*41, 42*). Bacterial cells can communicate with each other by means of a process called *quorum sensing* and detect when they are assembled in large numbers as opposed to when they are essentially alone (*43*). According to this theory, bacteria may secrete and sense small signaling molecules to communicate and to promote biofilm formation. Kim et al. (*40*) observed that the *E. coli* O157:H7 strain used in this study possessed extracellular materials outside the cell surface, which may initiate cell adhesion and contribute to cell−cell interactions.

The electrophoretic mobility of the *E. coli* O157:H7 cells was approximately $-0.15\ \mu m\ V\ s^{-1}\ cm^{-1}$ over the considered range of pH and IS (Table 1). Under these conditions with near-neutral surface charge, DLVO theory predicts the potential for cell−cell interactions. Additional support for cell−cell interactions was obtained from micromodel experiments. In a micromodel experiment conducted at pH 8.4 and 1 mM, the bacteria were found to preferentially coat sand grains (Figure 3). Once the coated sand grain was gently shaken, however, all the bacteria came off, indicating that the cell−cell interactions were weak enough to lead to release by physical perturbation.

Our previous study demonstrated that aggregation of *E. coli* O157:H7 cells occurred at pH 5.8, and that the aggregation rate increased with IS (0.01 to 100 mM) (*44*). This finding was confirmed with two flow interruptions at the end of the column experiment conducted in pH 5.8 and 1 mM. Cells that are weakly associated with the sand and/or retain in zones of relative flow stagnation within the pore structure should be released by Brownian diffusion during a flow interruption (*45, 46*). However, Figure 1 and Table 1 indicate that a negligible amount of cells (0.4%) were recovered during each flow interruption. In contrast, 39% of the total cells were recovered from this same system after removing the pore structure (Table 1). This result indicates that the cells were reversibly retained within the porous media, likely in an aggregated form that could not diffuse out during the flow interruption. Furthermore, mass balance information presented in Table 1 indicates that the irreversible and reversible fractions of cell retention changed with the pH and IS. Specifically, irreversible cell retention tended to increase with decreasing pH and IS, as a result of achieving more favorable attachment conditions. Reversible cell retention tended to became the dominant mechanism of cell retention under increasingly unfavorable attachment conditions (increasing pH and IS). In this case, SI Figures S4e and S4f demonstrate that minimal cell retention occurred in the pH 9.2 and 100 mM system, and that the cell retention was controlled by the pore structure. Additional evidence for cell−cell interactions and pore structure effects is provided below.

The shape of the BTCs presented in Figure 1 indicates that a variety of time dependent deposition processes were also occurring during these experiments. Continued increase in the effluent concentrations after breakthrough of the cells was observed for some systems (pH 8.4 and 10 mM, and pH 9.2 and 1 mM) and suggests a decreasing deposition rate as a function of time, presumably due to a blocking/filling effect (*5, 47*) or simultaneous attachment and detachment (*48*).

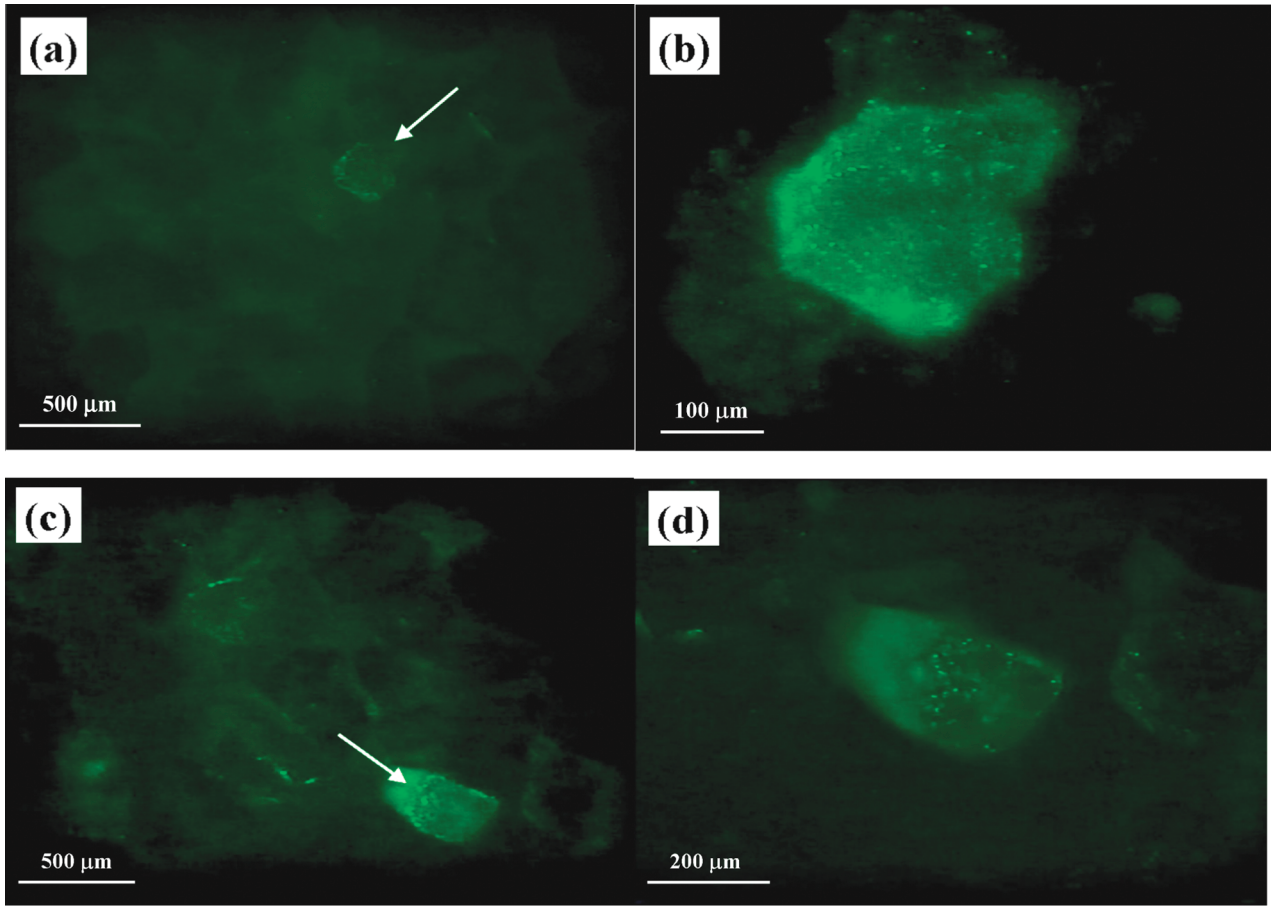

FIGURE 3. Microscope images of *E. coli* O157:H7 cells deposited on quartz grains: (a) 75×; (b) 300×; (c) 75×; and (d) 200× magnification. The experiment was conducted at pH 8.4 and IS 1 mM. The images were taken at two different locations (a and b at one location, and c and d at the other location, respectively). In (a) and (c), white arrows point out the quartz grains which were preferentially coated with bacteria. In (b) and (d), high magnification images of the quartz grains indicated by the arrows in (a) and (c) were presented.

The opposite trend (decrease in effluent concentration with continued addition of cells) was observed for the pH 8.4 and IS 100 mM system and indicates the potential of cell−cell interactions (*49, 50*) in the porous media. Based on the cell BTCs shown in Figure 1, it is logical to infer that steric stabilization of the surface macromolecules would decrease the strength of cell−cell interactions with increasing pH and IS. Comparison of the cell BTCs at pH 8.4 and 9.2 and IS of 100 mM supports this hypothesis. Specifically, a ripening (i.e., cell−cell interaction) was observed for the BTC at the lower pH condition (pH 8.2), but not at the higher pH condition (pH 9.2). The different degree of electrosteric stabilization with pH could be explained by changes in the separation distance of polymeric layers on the surfaces of cells; i.e., a larger separation at higher pH occurs due to the conformational changes of macromolecules by the changing extent of deprotonation of functional groups (*9, 51*).

Numerical modeling of the cell BTCs at pH 8.4 and 9.2 was conducted to gain additional insight on the mechanisms of cell retention under unfavorable attachment conditions. Fitted model parameters are shown in SI Table S2. The model provided a reasonable description of the BTCs ($r^2 > 0.744$). At a given IS, the deposition coefficient decreased with pH. This observation is consistent with DLVO predictions and measured changes in the sand zeta potential. Conversely, the deposition coefficient decreased and the release coefficient tended to increase with IS (at a given pH). This trend is attributed to pH-associated electrosteric stabilization of the cell surface macromolecules as discussed above. Fitted values of the maximum solid phase concentration of retained cells demonstrated that only a small fraction of the quartz surface area contributed to cell retention (i.e., 2−23%), and that this fraction decreased with IS and pH. This trend is unlikely due to chemical heterogeneity since thoroughly cleaned ultrapure quartz was used in this study. Instead, this observation supports the potential importance of pore structure in cell retention. A number of studies have recently demonstrated that retention in low velocity regions that occur near grain−grain junctions and/or in small pore spaces may significantly contribute to colloidal/microbial deposition in porous media under unfavorable attachment conditions (e.g., refs *5* and *52−54*). Furthermore, the fraction of the solid surface area contributing to cell retention in these locations has been demonstrated to increase with the adhesive force (*55, 56*); e.g., the solution chemistry. As the small fraction of the surface area that contributes to cell retention fills, the deposition rates decreases with time and the BTCs shown in Figure 1 therefore exhibit a time-dependent shape. When cell retention is confined to small fractions of the surface area the cells may interact with each other within these regions and aggregate. For example, Bradford et al. (*5*) observed nonmonotonic deposition profiles for *E. coli* O157:H7 and cell aggregates in aquifer sand under unfavorable attachment conditions. These authors attributed the nonmonotonic deposition profiles to the release and re-entrapment of the cells, which were initially deposited and aggregated near grain−grain contacts.

Implications. In this study, we demonstrated that *pH-associated electrosteric stabilization* can explain the observed trend of decreasing deposition of *E. coli* O157:H7 cells to

quartz sand with increasing IS (1−100 mM) under higher pH conditions (i.e., 8.4 and 9.2). One important implication of this mechanism is that previous work may have underestimated *E. coli* O157:H7 travel distances at higher salt and pH conditions in typical groundwater environments (i.e., pH 6−9 and IS 1−50 mM). This study also provides insight into the role of solution chemistry on *E. coli* O157:H7 fate and the impact of pH-induced electrosteric stabilization. It should be mentioned that the *E. coli* O157:H7 strain used in this study is not representative for all other pathogenic *E. coli* strains, and therefore the results may vary between cell strains as observed from other studies (e.g., refs *57*−*60*), indicating that species variation could be important. Nevertheless the findings in this work demonstrate some potentially important factors that are typically neglected in classic microbial interaction studies. This finding can help guide the design and efficient development of processes for the removal of the *E. coli* O157:H7 cells during soil passage such as sand/riverbank filtration, and infiltration trenches and basins.

Acknowledgments

This research was funded by the USDA CSREES NRI (2006−02541). The *E. coli* O157:H7/pGFP strain 72 was provided by Dr. Pina Fratamico (USDA-ARS-ERRC, Wyndmoor, PA). We acknowledge Alan Nguyen for assistance with micromodel experiments.

Supporting Information Available

Additional methods (experiments and numerical modeling), discussion (hydrophobic interactions and anion valence effect), and data pertaining to the viability, size, aspect ratio, electrophoretic mobility, and hydrophobicity of *E. coli* O157:H7 cells, zeta potentials of quartz sand as a function of pH and IS, micromodel experimental results conducted at four representative conditions, and fitted model parameters.This material is available free of charge via the Internet at http://pubs.acs.org.

Literature Cited

(1) Stevik, T. K.; Aa, K.; Ausland, G.; Hanssen, J. F. Retention and removal of pathogenic bacteria in wastewater percolating through porous media: a review. *Water. Res.* **2004**, *38*, 1355–1367.

(2) Law, D. Virulence factors of *Escherichia coli* O157:H7 and other Shiga toxin-producing *E. coli*. *J. Appl. Microbiol.* **2000**, *88*, 729–745.

(3) Mead, P. S.; Slutsker, L.; Dietz, V.; McCaig, L. F.; Bresee, J. S.; Shapiro, C.; Griffin, P. M.; Tauxe, R. V. Food-related illness and death in the United States. *Emerging Infect. Dis.* **1999**, *5*, 607–625.

(4) Armstrong, G. L.; Hollingsworth, J.; Morris, Jr, J. G. Emerging foodborne pathogens: *Escherichia coli* O157:H7 as a model of entry of a new pathogen into the food supply of the developed world. *Epidemiol. Rev.* **1996**, *18*, 29–51.

(5) Bradford, S. A.; Simunek, J.; Walker, S. L. Transport and straining of *E. coli* O157:H7 in saturated porous media. *Water Resour. Res.* **2006**, *42*, W12S12, DOI: 10.1029/2005WR004805.

(6) Fontes, D. E.; Mills, A. L.; Hornberger, G. M.; Herman, J. S. Physical and chemical factors influencing transport of microorganisms through porous media. *Appl. Environ. Microbiol.* **1991**, *57*, 2473–2481.

(7) Derjaguin, B. V.; Landau, L. D. *Acta Physicochim. U.S.S.R.* **1941**, *14*, 300.

(8) Verwey, E. J. W.; Overbeek, J. T. G. *Theory of the Stability of Lyophobic Colloids: The Interaction of Sol Particles Having an Electric Double Layer*; Elsevier: Amsterdam. 1948.

(9) Van Oss, C. J. *Interfacial Forces in Aqueous Media*; Marcel Dekker: New York, 1994.

(10) Dong, H.; Onstott, T. C.; DeFlaun, M. F.; Fuller, M. E.; Scheibe, T. D.; Streger, S. H.; Rothmel, R. K.; Mailloux, B. J. Relative dominance of physical versus chemical effects on the transport of adhesion-deficient bacteria in intact cores from South Oyster, Virginia. *Environ. Sci. Technol.* **2002**, *36*, 891–900.

(11) Dong, H.; Onstott, T. C.; DeFlaun; Ko, C.-H.; Hollingsworth, A. D.; Brown, D. G.; Mailloux, B. J. Theoretical prediction of collision efficiency between adhesion-deficient bacteria and sediment grain surface. *Colloid Surf. B.* **2002**, *24*, 229–245.

(12) Walker, S. L.; Redman, J A.; Elimelech, M. Role of cell surface lipopolysaccharides in *Escherichia coli* K12 adhesion and transport. *Langmuir* **2004**, *20*, 7736–7746.

(13) Tsuneda, S.; Aikawa, H.; Hayashi, H.; Yuasa, A.; Hirata, A. Extracellular polymeric substances responsible for bacterial adhesion onto solid surface. *FEMS Microbiol. Lett.* **2003**, *223*, 287–292.

(14) Prince, J. L.; Dickinson, R. B. Kinetics and forces of adhesion for a pair of capsular/unencapsulated staphylococcus mutant strains. *Langmuir.* **2003**, *19*, 154–159.

(15) Kuznar, Z. A.; Elimelech, M. Cryptosporidium oocyst surface macromolecules significantly hinder oocyst attachment. *Environ. Sci. Technol.* **2006**, *40*, 1837–1842.

(16) Considine, R. F.; Dixon, D. R.; Drummond, C. J. Laterally-resolved force microscopy of biological microspheres-Oocysts of *Cryptosporidium parvum*. *Langmuir.* **2000**, *16*, 1324–1330.

(17) Abu-Lail, N. I.; Camesano, T. A. Role of lypopolysaccharides in the adhesion, retention, and transport of *Escherichia coli* JM109. *Environ. Sci. Technol.* **2003**, *37*, 2173–2183.

(18) Burks, G. A.; Velegol, S. B.; Paramonova, E.; Lindenmuth, B. E.; Feick, J. D.; Logan, B. E. Macroscopic and nanoscale measurements of the adhesion of bacteria with varying outer layer surface composition. *Langmuir.* **2003**, *19*, 2366–2371.

(19) Rijnaarts, H. H. M.; Norde, W.; Bouwer, E. J.; Lyklema, J.; Zehnder, A. J. B. Reversibility and mechanism of bacterial adhesion. *Colloid Surf. B.* **1995**, *4*, 5–22.

(20) Rijnaarts, H. H. M.; Norde, W.; Lyklema, J.; Zehnder, A. J. B. DLVO and steric contributions to bacterial deposition in media of different ionic strengths. *Colloid Surf. B.* **1999**, *14*, 179–195.

(21) Williams, V.; Fletcher, M. *Pseudomonas fluorescens* adhesion and transport through porous media are affected by lipopolysaccharide composition. *Appl. Environ. Microbiol.* **1996**, *62*, 100–104.

(22) Kuznar, Z. A.; Elimelech, M. Role of surface proteins in the deposition kinetics of *Cryptosporidium* oocysts. *Langmuir* **2005**, *21*, 710–716.

(23) Gargiulo, G.; Bradford, S.; Simunek, J.; Ustohal, P.; Vereecken, H.; Klumpp, E. Bacteria transport and deposition under unsaturated conditions: The role of the matrix grain size and the bacteria surface protein. *J. Contam. Hydrol.* **2007**, *92*, 255–273.

(24) Considine, R. F.; Dixon, D. R.; Drummond, C. J. Oocysts of *Cryptosporidium parvum* and model sand surfaces in aqueous solutions: an atomic force microscope (AFM) study. *Water Res.* **2002**, *36*, 3421–3428.

(25) Chen, G.; Walker, S. L. Role of solution chemistry and ion valence on the adhesion kinetics of groundwater and marine bacteria. *Langmuir* **2007**, *23*, 7162–7169.

(26) Kuznar, Z. A.; Elimelech, M. Adhesion kinetics of viable *Cryptosporidium parvum* oocysts to quartz surfaces. *Environ. Sci. Technol.* **2004**, *38*, 6839–6845.

(27) Li, J.; McLandsborough, L. A. The effects of the surface charge and hydrophobicity of *Escherichia coli* on its adhesion to beef muscle. *Int. J. Food Microbiol.* **1999**, *53*, 185–193.

(28) Walker, S. L.; Redman, J. A.; Elimelech, M. Influence of growth phase on bacterial deposition: Interaction mechanisms in packed-bed column and radial stagnation point flow systems. *Environ. Sci. Technol.* **2005**, *39*, 6405–6411.

(29) Jester, W. A.; Briceno, M.; Jarrett, A. R.; Sakuma, S. H.; Yu, C. Evaluation of lanthanum and praseodymium chelates of DTPA, CDTA, EDTA, and NTA as groundwater tracers. *J. Radioanal. Nucl. Chem.* **1987**, *110*, 215–220.

(30) Mays, L. W. *Water Resources Handbook*. McGraw-Hill: Upper Saddle River, NJ, 1996.

(31) Delory, G. E.; King, E. J. A sodium carbonate-bicarbonate buffer for alkaline phosphatases. *Biochem. J.* **1945**, *39*, 245.

(32) Elimelech, M.; Nagai, M.; Ko, C.-H.; Ryan, J. N. Relative insignificance of mineral grain zeta potential to colloids transport in geochemically heterogeneous porous media. *Environ. Sci. Technol.* **2000**, *34*, 2143–2148.

(33) Bradford, S. A.; Simunek, J.; Bettahar, M.; Tadassa, Y. F.; van Genuchten, M. T.; Yates, S. R. Straining of colloids at textural interfaces. *Water Resour. Res.* **2005**, *41*, W10404, DOI: 10.1029/2004WR003675.

(34) Simunek, J.; van Genuchten, M. Th.; Sejna, M. *The HYDRUS-1D Software Package for Simulating the One-Dimensional Movement of Water, Heat, And Multiple Solutes in Variably-Saturated Media-Version 4.09*, HYDRUS Software Series 1; Department of

Environmental Science, University of California—Riverside: Riverside, CA.
(35) Yao, K. M.; Habibian, M. T.; O'Melia, C. R. Water and waste water filtration: Concepts and applications. *Environ. Sci. Technol.* **1971**, *5*, 1105–1112.
(36) Bradford, S. A.; Bettahar, M.; Simunek, J.; van Genuchten, M. T. Straining and attachment of colloids in physically heterogeneous porous media. *Vadose Zone J.* **2004**, *3*, 384–394.
(37) Redman, J. A.; Walker, S. L.; Elimelech, M. Bacterial adhesion and transport in porous media: Role of the secondary energy minimum. *Environ. Sci. Technol.* **2004**, *38*, 1777–1785.
(38) Jewett, D. G.; Hilbert, T. A.; Logan, B. E.; Arnold, R. G.; Bales, R. C. Bacterial transport in laboratory columns and filters: Influence of ionic strength and pH on collision efficiency. *Water Res.* **1995**, *29*, 1673–1680.
(39) Elimelech, M.; Gregory, J.; Jia, X.; Williams, R. A. *Particle Deposition and Aggregation: Measurement, Modeling and Simulation*; Butterworth-Heinemann: Oxford, England, 1995.
(40) Kim, H. N.; Hong, Y.; Lee, I.; Bradford, S. A.; Walker, S. L. Surface characteristics and adhesion behavior of *Escherichia coli* O157:H7: Role of extracellular macromolecules. *Biomacromolecules*, in review.
(41) Oh, Y. J.; Jo, W.; Yang, Y.; Park, S. Biofilm formation and local electrostatic force characteristics of *Escherichia coli* O157:H7 observed by electrostatic force microscopy. *Appl. Phys. Lett.* **2007**, *90*, 143901.
(42) Oh, Y. J.; Jo, W.; Yang, Y.; Park, S. Influence of culture conditions on *Escherichia coli* O157:H7 biofilm formation by atomic force microscopy. *Ultramicroscopy* **2007**, *107*, 869–874.
(43) Parsek, M. R.; Greenberg, E. P. Acyl-homoserin lactone quorum sensing in Gram-negative bacteria: A signaling mechanism involved in associations with higher organisms. Colloquium paper. *Proc. Natl. Acad. Sci.* **2000**, *97*, 8789–8793.
(44) Kim, H. N.; Walker, S. L.; Bradford, S. A. Macromolecule mediated transport and retention of *Escherichia coli* O157:H7 in saturated porous media. *Water Res.* submitted.
(45) Shen, C.; Li, B.; Huang, Y.; Jin, Y. Kinetics of coupled primary- and secondary-minimum deposition of colloids under unfavorable chemical conditions. *Environ. Sci. Technol.* **2007**, *41*, 6976–6982.
(46) *Soil-Water-Solute Process Characterization*; Javier Á.-B.; Rafael M.-C., Eds.; CRC Press: Boca Raton, FL, 2005.
(47) Camesano, T. A.; Unice, K. M.; Logan, B. E. Blocking and ripening of colloids in porous media and their implications for bacterial transport. *Colloids Surf. A* **1999**, *160*, 291–308.
(48) Tong, M.; Li, X.; Brow, C. N.; Johnson, W. P. Detachment-influenced transport of an adhesion-deficient bacterial strain within water-reactive porous media. *Environ. Sci. Technol.* **2005**, *39*, 2500–2508.
(49) Liu, D.; Johnson, P. R.; Elimelech, M. Colloid deposition dynamics in flow through porous media: Role of electrolyte concentration. *Environ. Sci. Technol.* **1995**, *29*, 2963–2973.
(50) Nascimento, A. G.; Totola, M. R.; Souza, C. S.; Borges, M. T.; Borges, A. C. Temporal and spatial dynamics of blocking and ripening effects on bacterial transport through a porous system: A possible explanation for CFT deviation. *Colloid Surf. B.* **2006**, *53*, 241–244.
(51) Grasso, D.; Subramaniam, K.; Butkus, M.; Strevett, K.; Bergendahl, J. A review of non-DLVO interactions in environmental colloidal systems. *Rev. Environ. Sci. Bio/Technol.* **2002**, *1*, 17–38.
(52) Bradford, S. A.; Torkzaban, S.; Walker, S. L. Coupling of physical and chemical mechanisms of colloid straining in saturated porous media. *Water Res.* **2007**, DOI: 10.1016/j.watres.2007.03.030.
(53) Tufenkji, N.; Miller, G. F.; Ryan, J. N.; Harvey, R. W.; Elimelech, M. Transport of *Cryptosporidium oocysts* in porous media: role of straining and physicochemical filtration. *Environ. Sci. Technol.* **2004**, *38*, 5932–5938.
(54) Johnson, W. P.; Li, X.; Yal, G. Colloid retention in porous media: Mechanistic confirmation of wedging and retention in zones of flow stagnation. *Environ. Sci. Technol.* **2007**, *41*, 1279–1287.
(55) Torkzaban, S.; Tazehkand, S. S.; Walker, S. L.; Bradford, S. A. Transport and fate of bacteria in porous media: Coupled effects of chemical conditions and pore space geometry. *Water Resour. Res.* **2008**, *44*, W04403, DOI: 10.1029/2007WR006541.
(56) Torkzaban, S.; Bradford, S. A.; Walker, S. L. Resolving the coupled effects of hydrodynamics and DLVO forces on colloid attachment in porous media. *Langmuir* **2007**, *23*, 9652–9660.
(57) Haznedaroglu, B. Z.; Bolster, C. H.; Walker, S. L. The role of starvation on *Escherichia coli* adhesion and transport in saturated porous media. *Water Res.* **2008**, *42*, 1547–1554.
(58) Bolster, C. H.; Haznedaroglu, B. Z.; Walker, S. L. Diversity in cell properties and transport behavior among 12 different environmental *Escherichia coli* isolates. *J. Environ. Qual.* **2009**, *38*, 465–472.
(59) Morrow, J. B.; Stratton, R.; Yang, H.-H.; Smets, B. F.; Grasso, D. Macro- and nanoscale observations of adhesive behavior for several *E. coli* strains (O157:H7 and environmental isolates) on mineral surfaces. *Environ. Sci. Technol.* **2005**, *39*, 6395–6404.
(60) Castro, F. D.; Tufenkji, N. Relevance of nontoxigenic strains as surrogates for *Escherichia coli* O157:H7 in groundwater contamination potential: Role of temperature and cell acclimation time. *Environ. Sci. Technol.* **2007**, *41*, 4332–4338.

ES8026055